ORIGINAL RESEARCH

Overactivated MX1 Positive Natural Killer Cells Promote the Progression of Sepsis-Induced Acute Respiratory Distress Syndrome

Qingxiang Liu [1],*, Fei Peng[1],*, Haitao Liu[2],*, Qin Sun[1], Hui Chen[1], Xinyi Xu[1], Zihan Hu [1], Xing Zhou[1], Kai Jin [1], Jianfeng Xie[1], Yingzi Huang[1], Wei Huang[1], Yi Yang[1]

[1]Jiangsu Provincial Key Laboratory of Critical Care Medicine, Department of Critical Care Medicine, Zhongda Hospital, School of Medicine, Southeast University, Nanjing, 210009, People's Republic of China; [2]School of Life Science, Fudan University, Shanghai, 200000, People's Republic of China

*These authors contributed equally to this work

Correspondence: Wei Huang; Yi Yang, Email whuang@seu.edu.cn; yiyiyang2004@163.com

Background: Natural killer (NK) cells are key regulators of immune defense in sepsis-induced acute respiratory distress syndrome (ARDS), yet the characteristics of NK cell clusters in ARDS remain poorly understood.

Methods: A prospective and observational study enrolled septic patients with ARDS or not was conducted to determine the percentage of NK cells via flow cytometry. The transcriptomes of peripheral blood mononuclear cells (PBMCs) from healthy controls, patients with sepsis only, and patients with sepsis-induced ARDS were profiled. Vitro experiments were performed to confirm the mechanism mediating MX1$^+$NK cell infiltration.

Results: A total of 115 septic patients were analyzed, among whom 63 patients developed ARDS and 52 patients did not. Decreased NK percentages were found in sepsis with ARDS patients (%, 7.46±4.40 vs 11.65±6.88, P=0.0001) compared with sepsis-only patients. A lower percentage of NK cells showed a significant increase in 28-day mortality. Single-cell sequencing analysis revealed distinct characteristics of NK cells in sepsis-induced ARDS, notably the identification of a unique cluster defined as MX1$^+$NK cells. Flow cytometry analysis showed an elevated percentage of MX1$^+$NK cells specifically in individuals with sepsis-induced ARDS, compared with patients with sepsis only. Pseudo-time analysis showed that MX1$^+$NK cells were characterized by upregulation of type I interferon-induced genes and other pro-inflammatory genes. MX1$^+$NK cells can respond to type I interferons and secrete type I interferons themselves. Ligand–receptor interaction analysis also revealed extensive interaction between MX1$^+$NK cells and T/B cells, leading to an uncontrolled inflammatory response in ARDS.

Conclusion: MX1$^+$NK cells can respond to type I interferons and secrete type I interferons themselves, promoting the development of sepsis-induced ARDS. Interfering with the infiltration of MX1$^+$NK cells could be a therapeutic approach for this disease. Due to the limited sample size, a larger sample size was needed for further exploration.

Keywords: ARDS, inflammation, natural killer cells, sepsis

Background

Acute respiratory distress syndrome (ARDS) is a common and life-threatening clinical syndrome, which affects 3 million people worldwide and accounts for up to 10% of intensive care unit (ICU) admissions.[1] It is characterized by acute hypoxemia, diffused pulmonary, and reduced lung compliance. In a large prospective cohort study, sepsis originating from the lungs emerged as the most common risk factor, accounting for 46% of patients at risk for ARDS.[2] Despite recent progress in basic research and clinical trials of ARDS, its mortality remains high at 30%–40%.[3] The treatment of ARDS remains a challenge in the ICU. The exploration of the immune pathological mechanisms underlying ARDS is crucial for improving patient outcomes.

Natural killer (NK) cells, a subset of cytotoxic lymphocytes, are pivotal in immune surveillance against infections and cancer,[4] as well as modulating adaptive immune responses.[5] NK cells were reported to be the most important immune cell subtype for the prediction of severe lung diffusion impairment, releasing a significant amount of pro-inflammatory cytokines such as tumor necrosis factor (TNF)-α and interferon (IFN)-γ during ARDS.[6] In mouse models of ARDS induced by lipopolysaccharide, depletion of NK cells leads to decreased production of inflammatory cytokines and improved lung function.[7] Elevated NK cell levels in bronchoalveolar lavage fluid were linked to COVID-19-induced ARDS severity.[8,9] Dysregulated NK cells were associated with worse clinical outcomes in COVID-19 patients, with NF-κB implicated in ARDS regulation.[6,10] Since NK cells play a crucial role in ARDS, our understanding of the roles of their various subtypes in ARDS remains incomplete.

Single-cell RNA sequencing (scRNA-seq) is considered as the gold standard for transcriptomic profiling due to its ability to sequence transcripts in individual cells, offering detailed insights into diseases like ARDS.[11] Yale Jiang et al utilized scRNA-seq on peripheral blood mononuclear cells (PBMCs) from ARDS patients, revealing a decreased proportion of NK cells lacking the *IFNGR1* receptor.[12] Disease-specific subsets of immune cells may exhibit unique phenotypes and functions, potentially playing key roles in disease pathogenesis. Detecting these characteristic cells can provide crucial evidence for early ARDS diagnosis and enable timely intervention. However, the roles of NK cell clusters in ARDS remain unrecognized.

In this study, we first analyze the percentage of NK cells in septic patients to investigate their association with sepsis-induced ARDS. We then utilize scRNA-seq data to uncover NK cell cluster heterogeneity in septic patients with and without ARDS. We identify a distinct MX1$^+$NK cell subtype and its relevance to ARDS, offering potential insights for future therapeutic approaches for sepsis-induced ARDS.

Methods

Human Patients

Blood was collected from patients with sepsis within 24 hours of meeting the consensus clinical definition of sepsis.[13] The exclusion criteria included the following: patients younger than 18 years; pregnancy; patients with malignancy, or chronic viral infection, such as hepatitis B, C, or HIV; autoimmune diseases, use of corticosteroid therapy; or consent could not be obtained. All patients were evaluated after admission and administered therapy according to the 2016 international guidelines for the management of sepsis.[14] Healthy volunteers were recruited.

Cell

Interleukin-2 (IL-2) activated NK cells were obtained as follows: freshly isolated splenocytes from C57B6/L mice were incubated with MACS DX5-coupled beads (Miltenyi) and then the positive selection was used.[15] Collected DX5$^+$cells were cultured for 12 hours in RPMI 10% FBS with β-mercaptoethanol, sodium pyruvate (1 mM), Hepes (10 mM), nonessential MEM amino acids, and 1000UI/mL of IL-2 (Peprotech, USA). And 20 ng/mL IFN-α and the same volume of PBS were added to the media at the beginning.

Flow Cytometry

Whole blood samples were collected from patients after sepsis was diagnosed. Cells were stained with anti-CD45-Brilliant Violet 570™ (BioLegend), anti-CD3-FITC (BioLegend), and anti-CD56-PE (BioLegend). For MX1 and intracellular cytokine staining, 250uL blood from each sample was resuspended and incubated in RPMI 1640 culture medium containing 3% FBS (Mediatech). The cells were then stimulated with a cell activation cocktail (with Brefeldin A) (eBioscience) for 5 h at 37°C. Cells were stained with Zombie Aqua™ fixable viability kit (BioLegend), anti-CD45-Alexa Fluor®700 (BioLegend), anti-CD3-Percp-cy5.5 (BioLegend), and anti-CD56-FITC (BioLegend). After surface staining, fixation, and permeabilization, we used anti-MX1-AF647 (Abcam), and anti-IFN-α (Invitrogen). Brilliant Violet 421-conjugated donkey anti-rabbit IgG was used as the secondary antibody (BioLegend).

For mice NK cells, cells were stained with Zombie Aqua™ fixable viability kit (BioLegend), anti-NK 1.1-FITC (BioLegend) and anti-MX1 (Proteintech). Alexa Fluor 647-conjugated donkey anti-rabbit IgG was used as the secondary antibody

(BioLegend). Data were collected on the LSRFortessa[TM] flow cytometer (BD Biosciences) and NovocyteD3000 flow cytometer. Data were further analyzed using FlowJo software.

Single-cell RNA-Seq Analysis

The scRNA-seq data for patients with sepsis were downloaded from the Gene Expression Omnibus (GEO) database with the accession number: GSE151263. The scRNA-seq data for 3 healthy controls (HC) were downloaded from the GEO database with the accession number: GSE157007.

Quality controls, normalization, dimensionality reduction, and clustering of scRNA-seq data were performed using the Seurat package (version 4.3.0).[16] Uniform manifold approximation and projection (UMAP) was used to visualize the result of clustering. We performed cell communication analysis using CellChat (v1.6.1).[17] To re-cluster the NK cells, the "FindClusters" function (resolution = 0.3) was applied again and obtain 5 clusters. R package CytoTRACE v0.3.3 was used to calculate the CytoTRACE scores for NK cells. CytoTRACE scores range from 0 to 1, while higher scores indicate less differentiation.[18] To elucidate the developmental origins of NK clusters, we employed the Monocle algorithm (version 2.24.0).[19] NicheNet (version 1.1.1)[20] was employed for the prediction of ligands influencing transcriptomic changes in target cells. Gene-enrichment analysis of the identified genes obtained via the "FindMarkers" function was carried out using the Cluster Profiler package in R (version 4.6.0), for all differentially expressed genes with an average $\log_2$FC value above 1, and an adjusted p-value below 0.01. The gene ontology (GO) analysis is then used to evaluate the biological functions associated with the identified genes.[21] In our analysis, we used PROGENy to predict the activity of 14 signaling pathways.[22] To analyze transcription factor activity at the single-cell level, we employed the SCENIC algorithm.[23]

Statistics

All data were analyzed using GraphPad Prism 9.0 (GraphPad Software, San Diego, CA, USA). Continuous variables between the two groups were compared using Student's t-test or the Mann–Whitney U-test. Binary variables are presented as frequencies and were compared using the chi-square test or Fisher's exact test. The cutoff value was optimized using Youden's J statistic. The Log-rank test was used to analyze survival data. P was set at 0.05.

Result

The Percentage of NK Cells Decreased in Patients with Sepsis

To characterize the cell types and gene expression profiles of PBMCs in sepsis, the PBMCs were isolated from 7 septic patients and 3 controls. Among them, 4 patients had only sepsis, and 3 patients had sepsis with ARDS. Based on expression profiles, PBMCs were clustered for 7 cellular compositions, as shown by UMAP (Figure 1A). The identified immune cells included monocyte cells *(CSF1R)*, T cells *(CD3E)*, B cells *(CD19)*, plasma cells *(MZB1)*, NK cells *(KLRD1)*, neutrophils *(CSF3R)*, and platelet *(ITGA2B)* (Figure 1B and C). Every cell fraction was represented by a bar plot of each analyzed group and each sample (Figure 1D and E). There was a significant decrease in the frequency of NK cells in sepsis with ARDS compared to healthy controls (Figure 1F).

The Percentage of NK Cells Was Associated with Sepsis-Induced ARDS and 28-Day Mortality in Sepsis

To investigate the association between NK cells and sepsis-induced ARDS, we conducted a prospective and observational study that enrolled 115 septic patients, 63 of whom were diagnosed with sepsis-induced ARDS and 52 of whom without ARDS. There was no significant difference in age and BMI between the two groups. Lungs were the main site of infection (n = 33; 52%) in patients with sepsis-induced ARDS. These patients had higher SOFA score (10 ± 5 vs 7 ± 3, P=0.001), APACHE II score (22 ± 9 vs 19 ± 7, P=0.015), and 28-day mortality [23 (37%) vs 8 (15%), P=0.012] compared to sepsis-only patients (Supplementary Table 1).

The percentage of NK cells in the sepsis with ARDS group was significantly lower compared with sepsis only group (%, 7.46 ± 4.40 vs 11.65 ± 6.88, P=0.0001) (Figure 2A and B). A ROC curve was subsequently used to evaluate the predictability of the percentage of NK cells in ARDS development in patients with sepsis, which yielded an AuROC of
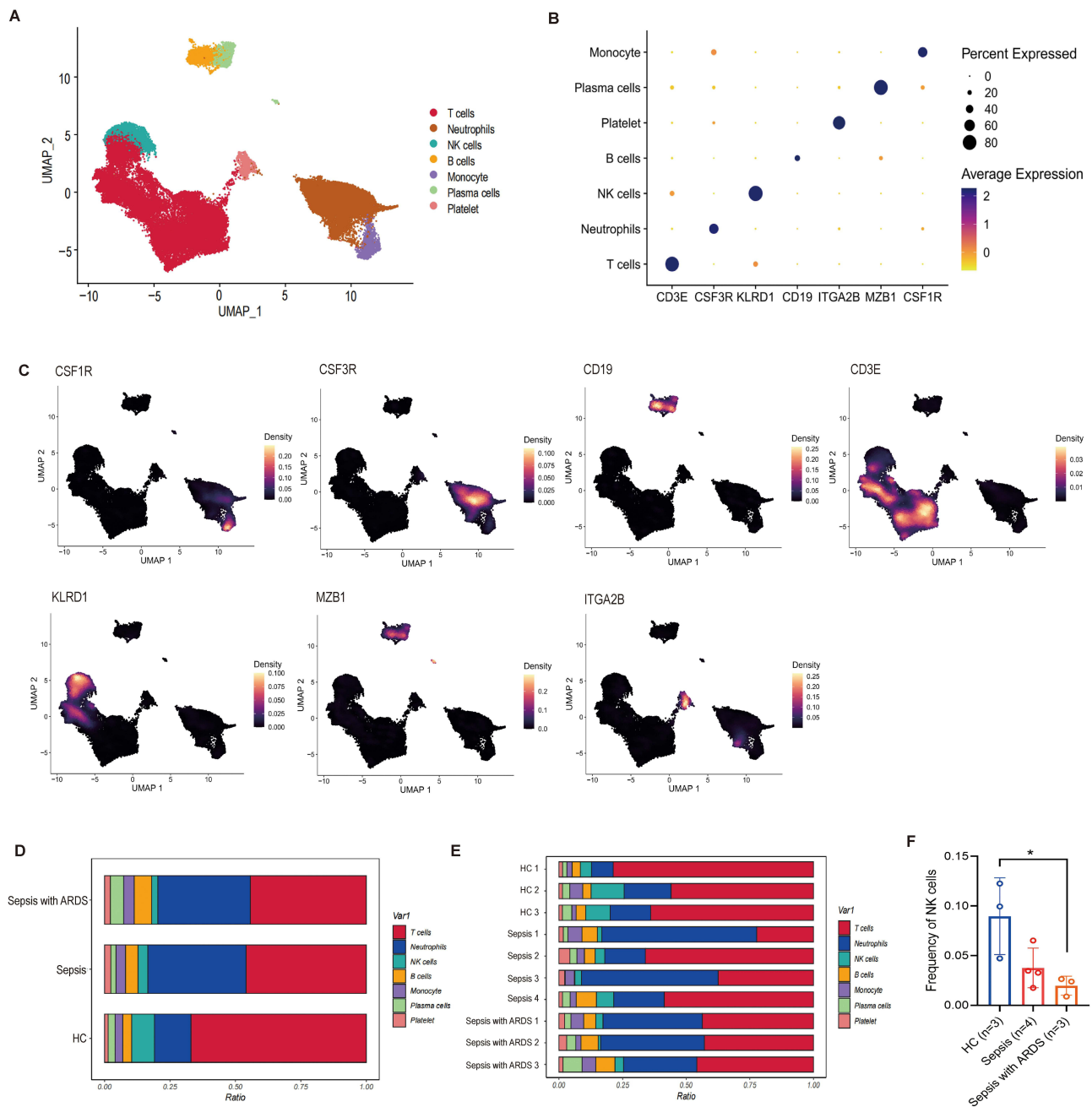
Figure 1 Cellular populations identified. (**A**) The UMAP plot displays the cellular composition. The UMAP projection of cells from HC (n=3), septic patients (n=4) and patients with sepsis-induced ARDS (n=3) shows the formation of 7 clusters with the respective labels. (**B** and **C**) Dotplot and UMAP show the marker gene expression in indicated cell types. (**D** and **E**) Bar plots indicate the proportion of cells in PBMC of different group and each analyzed patient. (**F**) Histograms indicate the frequencies of NK cells between HC group (n=3), sepsis group (n=4), and sepsis with ARDS group (n=3). The Student's t-test was performed. *P<0.05.

0.712 (95% CI: 0.620–0.792; P<0.001) (Figure 2D). A cutoff of 7.67% was calculated using the J statistics with a sensitivity of 65.08% and a specificity of 69.23%. And the percentage of NK cells in the 28-day survivors was significantly higher compared with non-survivors (%, 10.09 ± 6.42 vs 7.36 ± 4.17, P=0.030) (Figure 2C). A ROC curve was subsequently used to evaluate the predictability of the percentage of NK cells on 28-day mortality in patients with sepsis, which yielded an AuROC of 0.638 (95% CI: 0.543–0.725; P=0.020) (Figure 2E). A cutoff of 4.94% was calculated using the J statistics with a sensitivity of 41.94% and a specificity of 84.52%. Patients with a low percentage
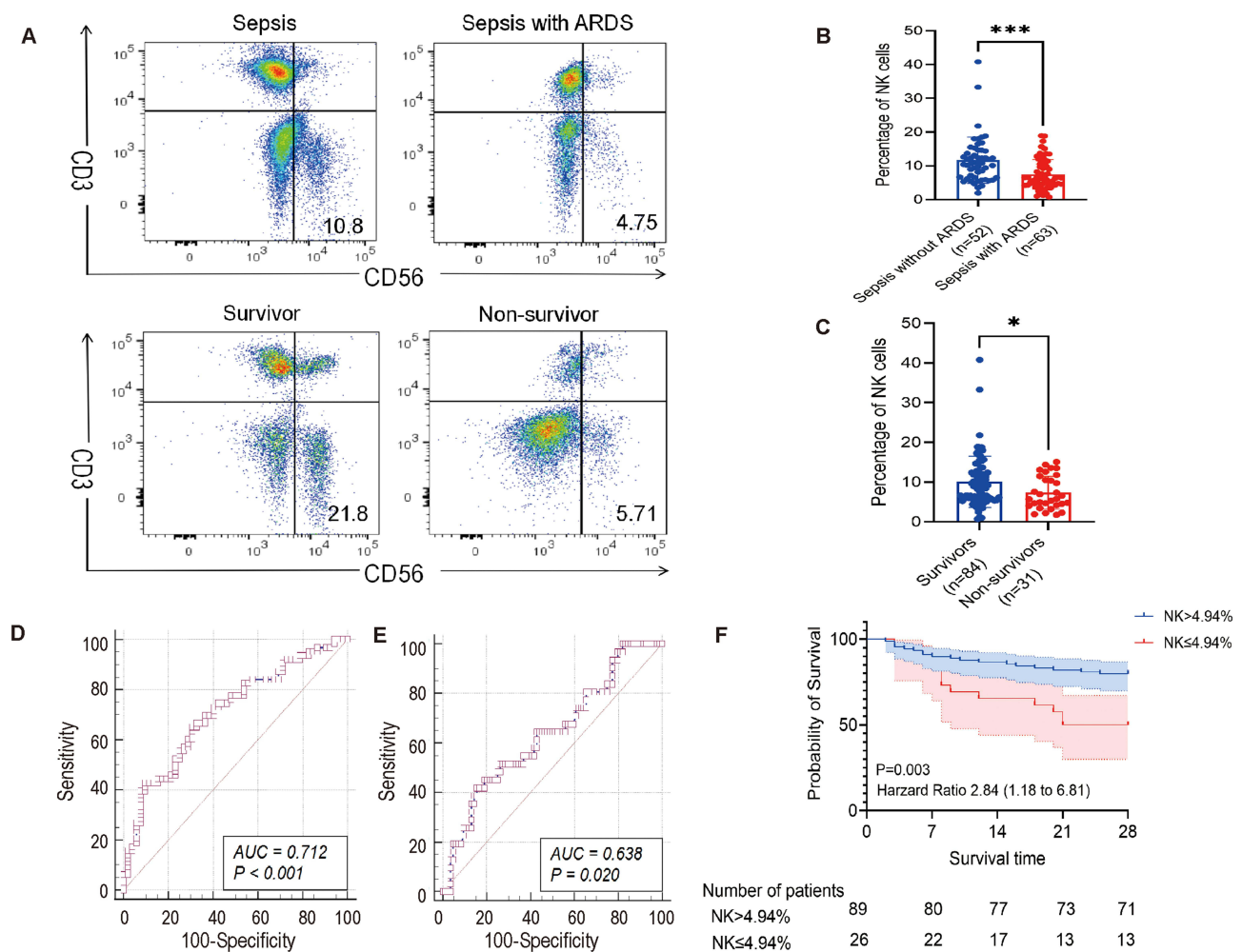
Figure 2 NK percentage was associated with ARDS development caused by sepsis and 28-day mortality in septic patients. (**A**) Representative flow cytometry graphs of NK cells. (**B**) Percentage of NK cells between septic patients with ARDS (n=63) and septic patients without ARDS (n=52). (**C**) Percentage of NK cells between 28-day non-survivors (n=31) and 28-day survivors (n=84). (**D**) ROC analysis of the percentage of NK cells predicting ARDS development in septic patients. (**E**) ROC analysis of the percentage of NK cells predicting 28-day mortality in septic patients. (**F**) Kaplan-Meier analysis of survival probability in septic patients with the percentage of NK cells >4.94% vs ≤4.94%. *$p<0.05$, ***$p<0.001$.

of NK cells showed significantly higher 28-day mortality (OR, 2.84; 95% CI, 1.18–6.81; $P=0.003$) (Figure 2F). Thus, NK cells play a significant role in the development of sepsis-induced ARDS.

## The Distinctive MX1⁺NK Cells in Patients with Sepsis-Induced ARDS

To comprehensively understand alterations in NK cell immune infiltration in ARDS, we conducted dimensionality reduction clustering of NK cells via unsupervised clustering. We used UMAP to visualize five distinct clusters (Figure 3A) and identified specific gene modules associated with each NK cell subgroup by visualizing the top 15 expressed genes (Figure 3C). These subgroups were characterized as MYOM2⁺NK, FOS⁺NK, GZMK⁺NK, S100A4⁺NK, and MX1⁺NK based on elevated expression of specific genes within each subgroup (Figure 3D). In the cohorts of HC, sepsis, and sepsis with ARDS, MYOM2⁺NK, FOS⁺NK, GZMK⁺NK, and S100A4⁺NK cells were consistently present. Notably, MX1⁺NK cells were exclusively detected in the sepsis with ARDS cohort (Figure 3B). We used flow cytometry to verify the expression of MX1⁺NK cells in HC, sepsis, and sepsis with ARDS. We found that MX1⁺NK cells were increased in sepsis with ARDS patients, but not sepsis, demonstrating that MX1⁺NK cells play an important role in the pathophysiology of sepsis-induced ARDS (Figure 3E and F), clinical characteristics of patients enrolled are listed in Supplementary Table 2.
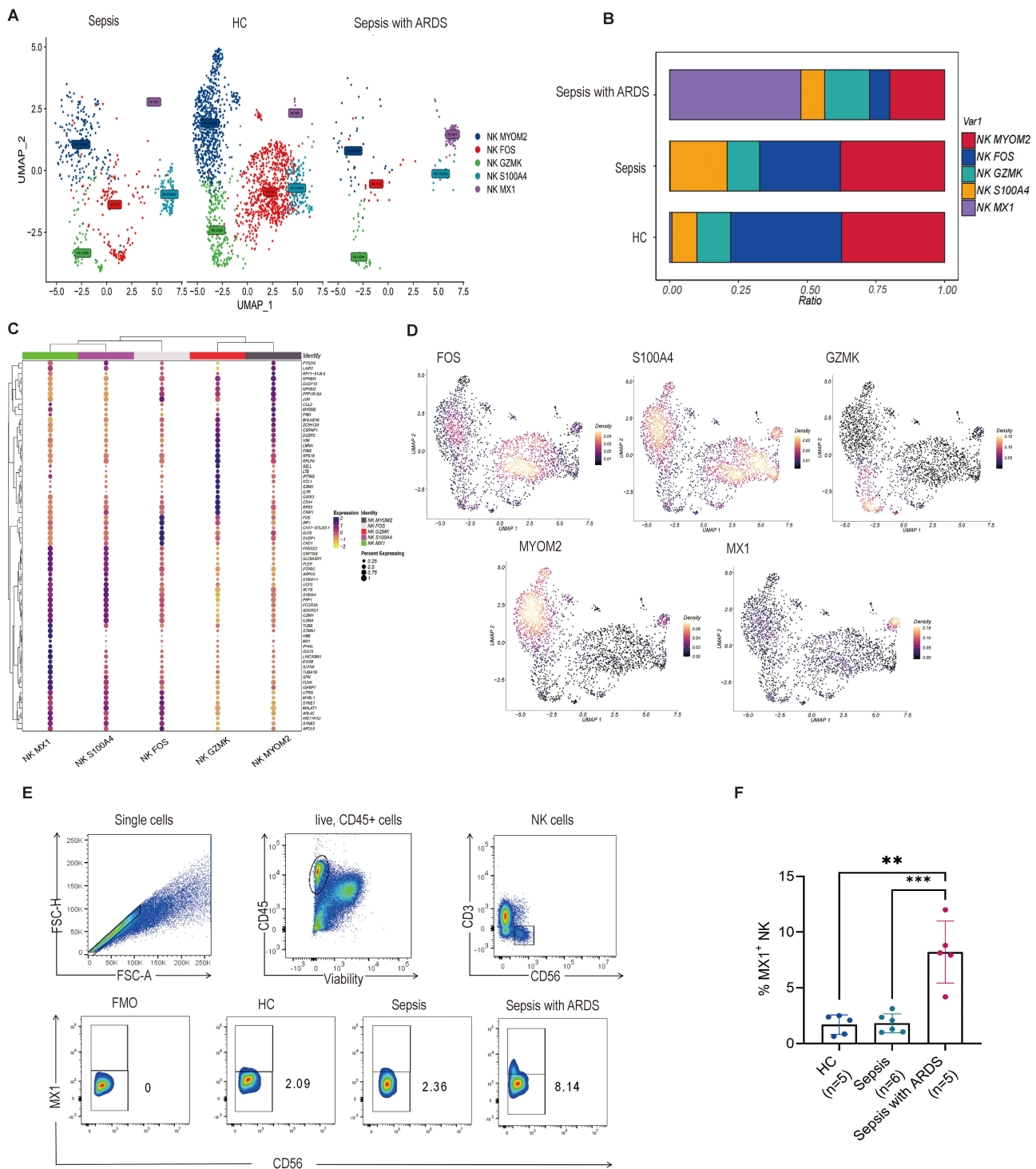
Figure 3 The distinctive MX1$^+$NK cells in patients with sepsis-induced ARDS. (**A**) The UMAP projection of NK cells from HC (n=3), patients with sepsis (n=4), and patients with sepsis-induced ARDS (n=3) show the formation of 5 clusters with the respective labels. (**B**) The average percentage of each cell type between HC, septic patients, and patients with ARDS. (**C** and **D**) Marker gene expression in NK subtypes. (**E**) Representative flow cytometry graphs of MX1$^+$NK cells. (**F**) Percentage of MX1$^+$NK cells between HC (n=5), patients with sepsis (n=6), and patients with sepsis-induced ARDS (n=5). The Student's t-test was performed. **P<0.01, ***P<0.001.

Pro-Inflammatory Properties of MX1$^+$NK Cells

Using cytoTRACE, we found that MX1$^+$NK cells exhibit the lowest predicted differentiation scores, suggesting that they represent a more advanced state of differentiation (Figure 4A–C). Pseudo-time analysis showed MX1$^+$NK cells primarily distributed in later stages (Figure 4D and E). The branching tree indicated these cell clusters did not bifurcate along the
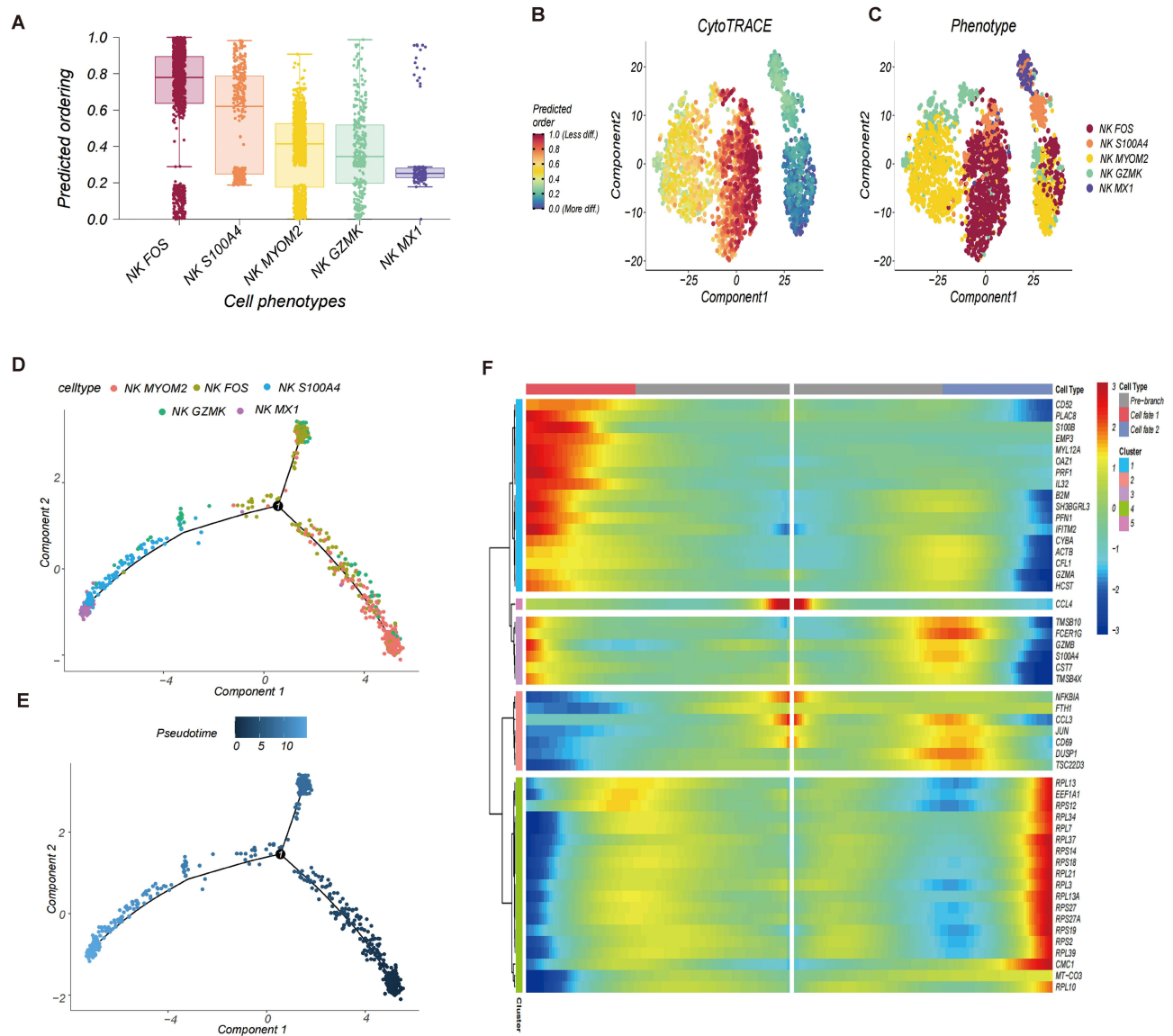
Figure 4 Pro-inflammatory properties of MX1⁺NK cells. (**A**) Ranking of cell differentiation according to CytoTRACE. (**B**) Differentiation trajectories obtained by CytoTRACE. (**C**) Distribution of 5 NK cell types. (**D** and **E**) The development trajectory of NK subsets is inferred by Monocle2. (**F**) The patterns of gene expression along with the pseudotime.

developmental trajectory, implying developmental continuity among the cell clusters. The branched heatmap displayed expression dynamics of the top 50 significant genes, showing a shift from ribosome biogenesis to a pro-inflammatory state as pseudo time progressed (Figure 4F). Increased expression of pro-inflammatory factors like *IL32, GZMB, GZMA*, and *S100A4* highlights MX1⁺NK cells' potential role in sepsis-induced ARDS.

MX1⁺NK Cells Promote the Development of ARDS Induced by Sepsis via IFN-α

To further explore the gene signature of MX1⁺NK cells, we visualized differential genes between MX1⁺NK cells and other clusters of NK cells. We found that MX1⁺NK cells highly expressed pro-inflammatory molecules, such as *GZMB, IL32, S100A9, CX3CR1,* and *PRF1* (Figure 5A). They play an important role in amplifying inflammatory responses, contributing to the pathogenesis of ARDS. To gain more functional insights into the genes expressed by MX1⁺NK cells in ARDS, GO analysis was conducted (Figure 5B), revealing associations with response to virus, positive regulation of
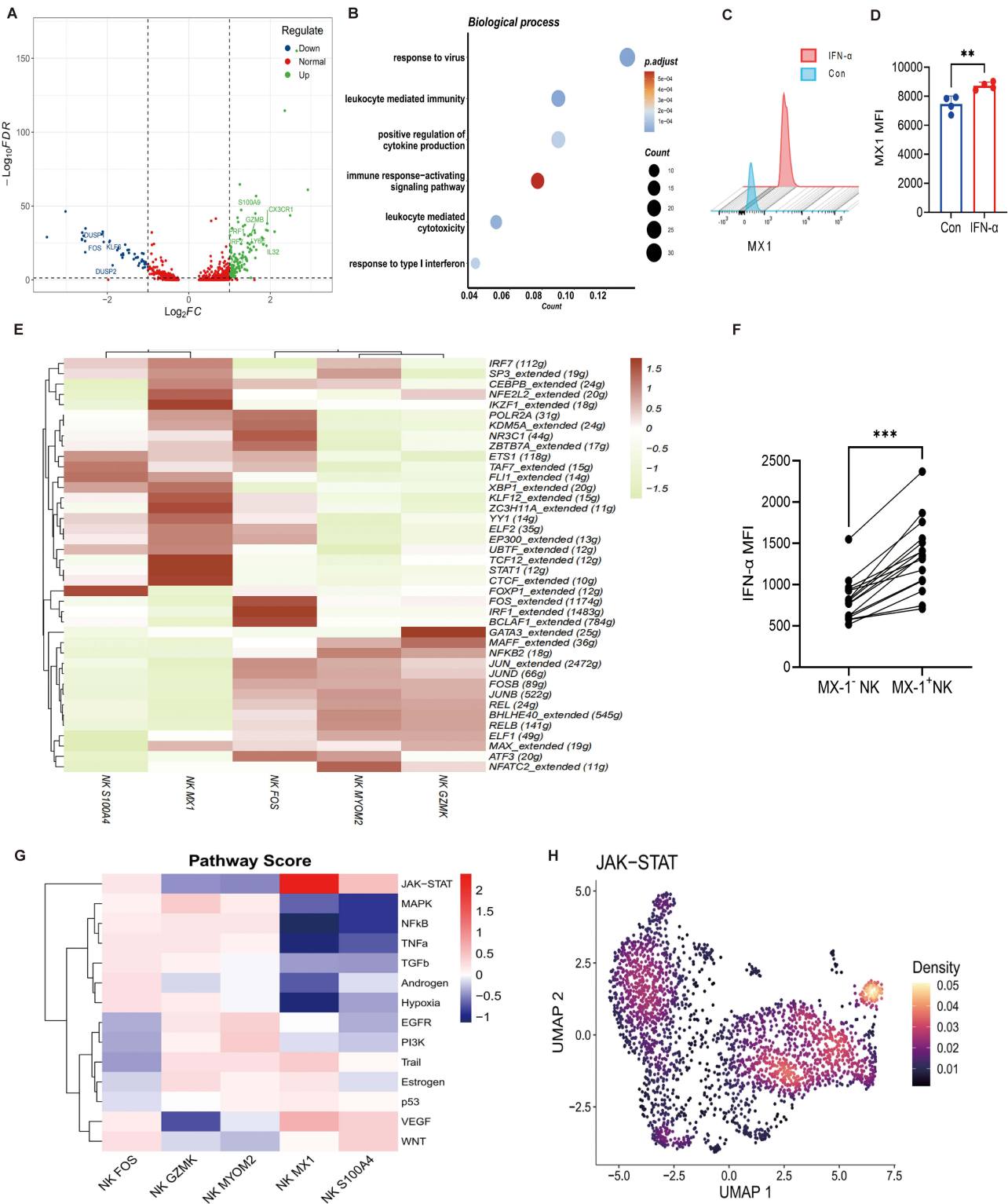
Figure 5 MX1^{+}NK cells promote the development of ARDS induced by sepsis via IFN-α. (**A**) The volcano plot shows differentially expressed genes between MX1^{+}NK cells from other NK cell subtypes. (**B**) Biological process of GO enrichment analysis. The words on the left indicate enriched terms and the color indicates the level of the enrichment. (**C**) Representative flow cytometry graphs of IFN-α MFI expressed by MX1^{+}NK cells and MX1^{−}NK cells. (**D**) NK cells respond to IFN-α stimulation. The Student's t-test was performed. **P<0.01. The experiments were repeated at least three times. (**E**) Heatmap shows NK cell subtypes transcription factor activity. (**F**) IFN-α MFI between MX1^{+}NK cells and MX1^{−}NK cells. The Student's t-test was performed. ***P<0.001. (**G**) Heatmap of 14 signal pathways activity. (**H**) The UMAP plot displays the expression of JAK-STAT.

cytokine production, and response to type I interferon. In vitro experiments demonstrated that IFN-α can induce the expression of *MX1* in NK cells (8709.0 ± 260.7 vs 7450.0 ± 565.9, P=0.007) (Figure 5C and D).

Transcription factor analysis revealed a significant enrichment of *IRF7* and *STAT1* in MX1+NK cells (Figure 5E). *IRF7* regulates interferon and interferon-stimulated gene expression, while *STAT1* mediates downstream signaling of type I/II interferons, cytokines, and growth factors. Clinical data showed higher IFN-α Mean Fluorescence Intensity (MFI) in MX1+NK cells compared to MX1−NK cells (1345.0 ± 426.4 vs 807.8 ± 253.7, P=0.0002) (Figure 5F). Additionally, pathway enrichment analysis using PROGENy revealed significant enrichment of the JAK-STAT pathway in MX1+NK cells (Figure 5G). Visualization via UMAP demonstrated high expression of JAK-STAT signaling in MX1+NK cells compared to other NK clusters (Figure 5H). Given its role in regulating immunity and other biological processes, the activation of the JAK-STAT pathway in MX1+NK cells offers valuable insights into their potential mechanism in ARDS.

The Regulatory Effect of MX1+NK Cells on T Cells During ARDS Induced by Sepsis

Activated NK cells can induce damage to lung epithelial and endothelial cells in ARDS by activating other immune cells such as T cells, macrophages, and B cells. Our analysis using Cellchat revealed extensive communications between MX1+NK cells and other immune cells (Figure 6A). Additionally, we investigated key ligand-receptor pairs sent from MX1+NK cells to other cell types in ARDS and compared them to control samples (Figure S1A and S1B).

The interaction between MX1+NK cells and T cells spans both innate and adaptive immunity. We subdivided T cells into six subgroups (Figure 6B). Effector CD8+T cells displayed high expression of *CD3E, CD8A, and GZMK*. Naive CD8+T cells expressed high levels of *CD3E, CD8A*, and *SELL*. NKT cells exhibited high expression of *CD3E and KLRF1*. Regulatory T cells demonstrated high expression of *CD4* and *FOXP3*. Naive CD4+T cells expressed high levels of *CD3E, CD4*, and *SELL*. Memory CD4+T cells expressed high levels of *CD3E, CD4*, and *ANXA1* (Figure 6D). A decrease in effector CD8+T cells and NKT cells was observed in ARDS compared to normal (Figure 6C). MX1+NK cells exhibited extensive interactions with various T cell subpopulations, including effector CD8+T cells, NKT cells, and Treg cells (Figure 6E). Cellchat analysis highlighted the enrichment of MIF-related ligand-receptor pairs between MX1+NK cells and T cells, particularly Treg cells, NKT cells, and memory CD4+T cells (Figure 6F). Additionally, IL-16-induced signaling implicated Treg cells and memory CD4+T cells as primary responders to IL-16 produced by MX1+NK cells (Figure 6G). Further analysis using "Nichenetr" revealed specific receptor-ligand pairs, such as TIGIT-CD226, CD27-CD70, and ITGB7-ITGA4 between MX1+NK cells and different T cell subtypes in ARDS (Figure 6H).

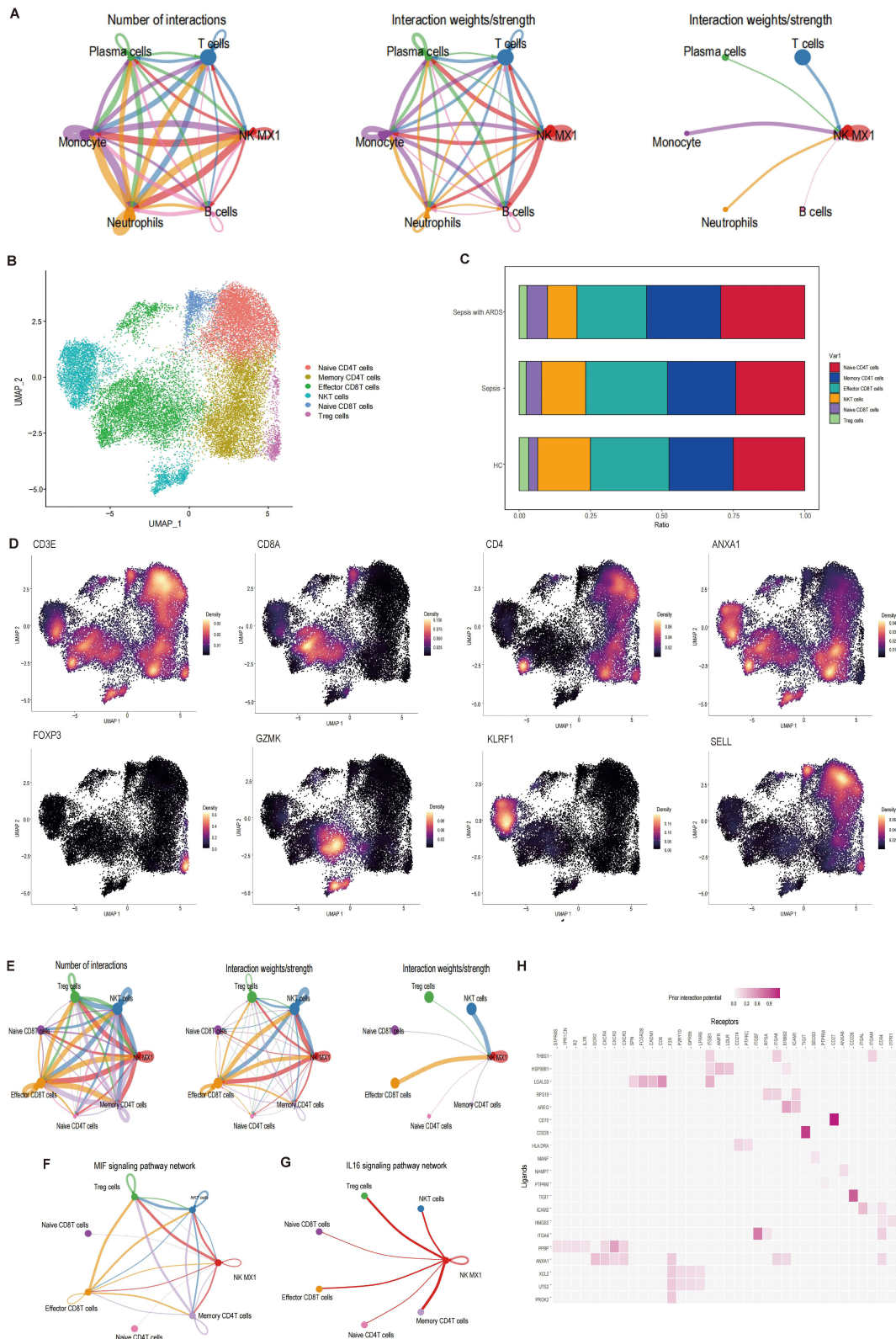## The Regulatory Effect of MX1+NK Cells on B Cells During ARDS Induced by Sepsis

To explore MX1+NK cell interactions with B cells, we categorized B cells into three subgroups (Figure 7A and B). Naive B cells expressed signature genes *IGHD, FCER2, TCL1A,* and *IL4R*, while memory B cells expressed *CD27, AIM2,* and *TNFRSF13B*, and plasma cells expressed *MZB1* and *JCHAIN* (Figure 7C). During ARDS, MX1+NK cells showed increased interactions with plasma cells but decreased interactions with memory B cells and naive B cells. Interaction strength was enhanced with all B cell subtypes in ARDS (Figure 7D). Specifically, CCL signaling increased from MX1+NK cells to naive B cells, memory B cells, and plasma cells in ARDS (Figure 7E), while Transforming growth factor-β (TGF-β) signaling decreased (Figure 7F). TGF-β-induced signaling indicated memory B cells and plasma cells as primary responders to TGF-β produced by MX1+NK cells (Figure 7G). TGF-β has immunosuppressive effects that restrain inflammatory processes, which inhibit lymphocyte proliferation and activity.

Discussion

The study provides novel insight into the pathophysiology of sepsis-induced ARDS, focusing on the NK cell heterogeneity and the role of MX1+NK cells. A prospective and observational clinical study revealed that reduced NK cells were correlated with sepsis-induced ARDS and worse outcomes in sepsis. ScRNA-seq analysis revealed NK cell heterogeneity in PBMCs of healthy volunteers, patients with only sepsis, and those with sepsis-induced ARDS, identifying pro-inflammatory MX1+NK cells in sepsis-induced ARDS.

MX1, a defining marker for MX1+NK cells, is highly expressed in sepsis-induced ARDS. It acts as an interferon-stimulated GTPase, crucial for anti-infection responses.[24] MX1+NK cells show enrichment of pro-inflammatory

Figure 6 The regulatory effect of MX1+NK cells on T cells during ARDS induced by sepsis. (**A**) Diagrams display the number of interactions and interaction strength in cell clusters in ARDS. (**B**) The UMAP projection of T cells shows the formation of 6 clusters with the respective labels. (**C**) The average percentage of each cell type between HC, septic patients, and patients with sepsis-induced ARDS. (**D**) Marker gene expression in T cell subtypes. (**E**) Diagrams display the number of interactions and interaction strength between MX1+NK cells and T cell subtypes in ARDS. (**F**) MIF mediating signaling pathway in ARDS. (**G**) IL-16 mediating signaling pathway in ARDS. (**H**) Heatmap shows the ligand-receptor pairs between MX1+NK cells and T cell subtypes.
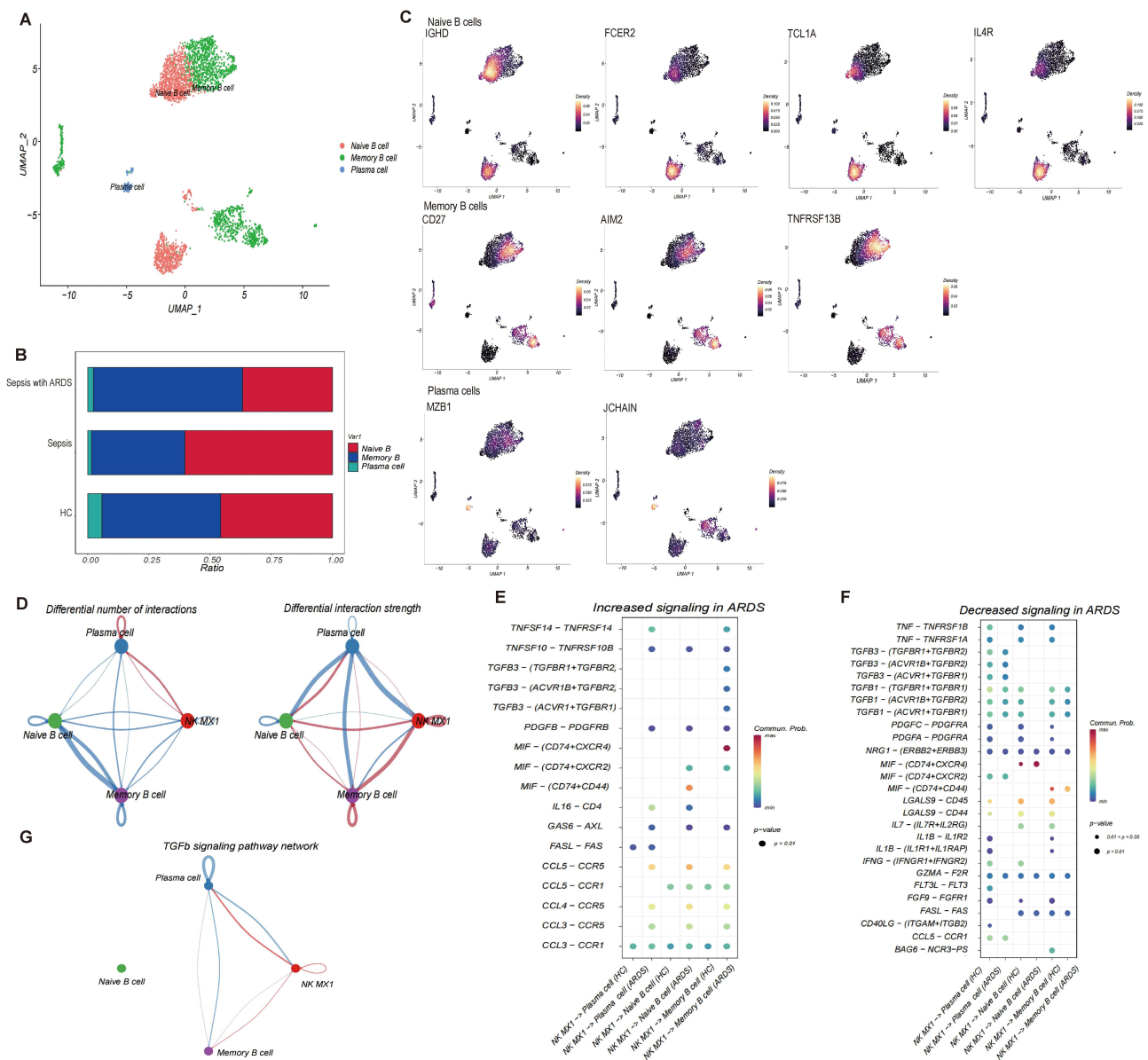
Figure 7 The regulatory effect of MX1$^+$NK cells on B cells during ARDS induced by sepsis. (**A**) The UMAP projection of B cells shows the formation of 3 clusters with the respective labels. Each dot corresponds to a single cell, colored according to cell type and group. (**B**) The average percentage of each cell type of B cells between HC, septic patients, and patients with sepsis-induced ARDS. (**C**) Marker gene expression in B cell subtypes. (**D**) Diagrams display the differential number of interactions and differential interaction strength between MX1$^+$NK cells and B cell subtypes in ARDS. (**E** and **F**) The communicated probability and related P values of the selected ligand-receptor interactions between MX1$^+$NK cells and B cell subtypes within the ARDS. Dot color reflects communication probabilities and dot size represents computed p-values. P < 0.05 refers to the significant ligand-receptor interaction. (**G**) TGFb mediating signaling pathway in ARDS.

cytokines and respond to type I interferons, forming a positive feedback loop leading to uncontrolled inflammation in ARDS. Schabmeyer et al found that type I interferons can induce *MX1* expression in a dose-dependent manner.[25] While type I IFNs are crucial for combating infections, uncontrolled and prolonged type I IFN signaling can be detrimental.[26] Yale Jiang also found extraordinarily high levels of type I IFN along with a sustained *IFN* gene signature in ARDS patients.[12] Thus, current evidence indicates that MX1$^+$NK cells respond to and produce type I IFN. Dysregulated type I IFN signaling via the JAK-STAT pathway promotes the development of ARDS.

NK cells exhibit rapid and nonspecific cytotoxic activities and secrete cytokines like IFN to amplify adaptive immune responses. Our study identified interactions between MX1$^+$NK cells and T/B cell subsets in ARDS. We found that the MIF-related signaling pathway and IL-16 pathway were involved in activating T cells and promoting inflammation.

Furthermore, the attenuation of TGF-β-induced signaling between MX1^{+}NK cells and plasma cells/memory B cells also indicates increased proinflammatory responses during ARDS. The sustained inflammatory response is a central feature in sepsis-induced ARDS pathogenesis. Interestingly, there were sex-specific variations observed in NK cell response in ARDS, yet the mechanisms underlying these differences remain unclear. Potential factors may involve sex-specific epigenetic modifications.[27–29]

Several limitations exist in our study. Firstly, the intracellular network regulatory mechanisms identified through cell-cell interaction analysis were not experimentally validated, since isolating different immune cell types and co-culturing them to study the interactions is challenging. Secondly, since our data was publicly available from the GEO database, it lacks detailed information regarding baseline characteristics of individual patients, we are unable to perform a comprehensive analysis. At last, due to the limited sample size, a larger sample size and the single-cell RNA sequencing data from alveolar lavage were needed for further exploration.

Conclusions

This study provides a novel perspective on the involvement of NK cells, particularly the distinct MX1^{+}NK cluster, in sepsis-induced ARDS. MX1^{+}NK cells can respond to type I interferons and secrete type I interferons themselves, promoting the development of ARDS induced by sepsis. MX1^{+}NK cells can serve as a biomarker for sepsis-induced ARDS, and interfering with the infiltration of MX1^{+}NK cells could be a therapeutic approach for this disease. Due to the limited sample size, a larger sample size was needed for further exploration.

Abbreviations

NK, Natural killer; ARDS, Acute respiratory distress syndrome; PBMC, Peripheral blood mononuclear cell; ICU, Intensive care unit; TNF-α, Tumor necrosis factor -α; IFN-γ, Interferon-γ; scRNA-seq, Single-cell RNA sequencing; GEO, Gene Expression Omnibus; UMAP, Uniform Manifold Approximation and Projection; GO, gene ontology; IL-2, Interleukin-2; TGF-β, Transforming growth factor -β; MFI, Mean fluorescence intensity; APACHE, Acute Physiology and Chronic Health Evaluation; SOFA, Sequential Organ Failure Assessment.

Data Sharing Statement

The scRNA-seq data of septic patients and healthy controls used in this study are publicly available from the GEO database under accession numbers GSE151263 and GSE157007. All data generated or analyzed during this study are included in this published article and its Supplementary Information Files.

Ethics Approval and Consent to Participate

The study was approved by the research ethics committee of Zhongda Hospital (Southeast University, Nanjing, China, approval ID: 2020ZDSYLL308-P01 and 2023ZDSYLL098-P01) and was in full compliance with the Declaration of Helsinki. Informed consent was obtained from each patient or their legal representative and healthy volunteers before enrollment in the study. All mouse procedures were performed under protocol guidelines approved by the Institutional Animal Care and Use Committee at the Medical School of Southeast University (approval ID:20190226003).

Funding

Disclosure

The authors have declared that no conflicts of interest exist in this work.

References

1. Bellani G, Laffey JG, Pham T, et al. Epidemiology, patterns of care, and mortality for patients with acute respiratory distress syndrome in intensive care units in 50 countries. *JAMA*. 2016;8(315):788–800. doi:10.1001/jama.2016.0291

2. Rubenfeld GD, Caldwell E, Peabody E, et al. Incidence and outcomes of acute lung injury. *N Engl J Med*. 2005;16(353):1685–1693. doi:10.1056/NEJMoa050333

3. Fan E, Brodie D, Slutsky AS. Acute respiratory distress syndrome: advances in diagnosis and treatment. *JAMA*. 2018;7(319):698–710. doi:10.1001/jama.2017.21907

4. Deng X, Terunuma H, Nieda M. Immunosurveillance of cancer and viral infections with regard to alterations of human NK cells originating from lifestyle and aging. *Biomedicines*. 2021;5(9). doi:10.3390/biomedicines9050557

5. Vivier E, Tomasello E, Baratin M, Walzer T, Ugolini S. Functions of natural killer cells. *Nat Immunol*. 2008;5(9):503–510. doi:10.1038/ni1582

6. Deng X, Terunuma H, Nieda M. Exploring the utility of NK cells in COVID-19. *Biomedicines*. 2022;5(10). doi:10.3390/biomedicines10051002

7. Zhou G, Juang SW, Kane KP. NK cells exacerbate the pathology of influenza virus infection in mice. *Eur J Immunol*. 2013;4(43):929–938. doi:10.1002/eji.201242620

8. Santinelli L, Lazzaro A, Sciarra F, et al. Cellular immune profiling of lung and blood compartments in patients with SARS-CoV-2 infection. *Pathogens*. 2023;3(12). doi:10.3390/pathogens12030442

9. Chen H, Liu W, Wang Y, Liu D, Zhao L, Yu J. SARS-CoV-2 activates lung epithelial cell proinflammatory signaling and leads to immune dysregulation in COVID-19 patients. *Ebiomedicine*. 2021;70:103500. doi:10.1016/j.ebiom.2021.103500

10. Zhang JY, Whalley JP, Knight JC, Wicker LS, Todd JA, Ferreira RC. SARS-CoV-2 infection induces a long-lived pro-inflammatory transcriptional profile. *Genome Med*. 2023;1(15):69. doi:10.1186/s13073-023-01227-x

11. Kan M, Shumyatcher M, Himes BE. Using omics approaches to understand pulmonary diseases. *Respir Res*. 2017;1(18):149. doi:10.1186/s12931-017-0631-9

12. Jiang Y, Rosborough BR, Chen J, et al. Single cell RNA sequencing identifies an early monocyte gene signature in acute respiratory distress syndrome. *JCI Insight*. 2020;13(5). doi:10.1172/jci.insight.135678

13. Singer M, Deutschman CS, Seymour CW, et al. The third international consensus definitions for sepsis and septic shock (Sepsis-3). *JAMA*. 2016;8(315):801–810. doi:10.1001/jama.2016.0287

14. Rhodes A, Evans LE, Alhazzani W, et al. Surviving sepsis campaign: international guidelines for management of sepsis and septic shock: 2016. *Intensive Care Med*. 2017;3(43):304–377. doi:10.1007/s00134-017-4683-6

15. Tomasello E, Desmoulins P, Chemin K, et al. Combined natural killer cell and dendritic cell functional deficiency in KARAP/DAP12 Loss-of-Function mutant mice. *Immunity*. 2000;3(13):355–364. doi:10.1016/S1074-7613(00)00035-2

16. Stuart T, Butler A, Hoffman P, et al. Comprehensive integration of Single-Cell data. *Cell*. 2019;7(177):1888–1902. doi:10.1016/j.cell.2019.05.031

17. Jin S, Guerrero-Juarez CF, Zhang L, et al. Inference and analysis of cell-cell communication using CellChat. *Nat Commun*. 2021;1(12):1088. doi:10.1038/s41467-021-21246-9

18. Gulati GS, Sikandar SS, Wesche DJ, et al. Single-cell transcriptional diversity is a hallmark of developmental potential. *Science*. 2020;6476(367):405–411. doi:10.1126/science.aax0249

19. Qiu X, Hill A, Packer J, Lin D, Ma YA, Trapnell C. Single-cell mRNA quantification and differential analysis with Census. *Nat Methods*. 2017;3(14):309–315. doi:10.1038/nmeth.4150

20. Browaeys R, Saelens W, Saeys Y. NicheNet: modeling intercellular communication by linking ligands to target genes. *Nat Methods*. 2020;2(17):159–162. doi:10.1038/s41592-019-0667-5

21. Zhou Y, Zhou B, Pache L, et al. Metascape provides a biologist-oriented resource for the analysis of systems-level datasets. *Nat Commun*. 2019;1(10):1523. doi:10.1038/s41467-019-09234-6

22. Schubert M, Klinger B, Klunemann M, et al. Perturbation-response genes reveal signaling footprints in cancer gene expression. *Nat Commun*. 2018;1(9):20. doi:10.1038/s41467-017-02391-6

23. Bravo GC, De Winter S, Hulselmans G, et al. SCENIC+: single-cell multiomic inference of enhancers and gene regulatory networks. *Nat Methods*. 2023;9(20):1355–1367. doi:10.1038/s41592-023-01938-4

24. Ghoreshi ZA, Abbasi-Jorjandi M, Asadikaram G, Sharifzak M, Rezazadeh-Jabalbarzi M, Rashidinejad H. Evaluation of MX1 gene promoter methylation in different severities of COVID-19 considering patient gender. *Clin Lab*. 2022;10(68). doi:10.7754/Clin.Lab.2022.220104

25. Schabmeyer ST, Kneidl AM, Schneider JK, et al. Concentration-Dependent type 1 Interferon-Induced regulation of MX1 and FABP3 in bovine endometrial explants. *Animals*. 2021;2(11). doi:10.3390/ani11020262

26. Tilg H, Kaser A. Interferons and their role in inflammation. *Curr Pharm Des*. 1999;10(5):771–785. doi:10.2174/1381612805666230111210939

27. Ghosh B, Chengala PP, Shah S, et al. Cigarette smoke-induced injury induces distinct sex-specific transcriptional signatures in mice tracheal epithelial cells. *Am J Physiol-Lung C*. 2023;4(325):L467–L476. doi:10.1152/ajplung.00104.2023

28. Phan M, Chun S, Kim S, et al. Natural killer cell subsets and receptor expression in peripheral blood mononuclear cells of a healthy Korean population: reference range, influence of age and sex, and correlation between NK cell receptors and cytotoxicity. *Hum Immunol*. 2017;2(78):103–112. doi:10.1016/j.humimm.2016.11.006

29. Cheng MI, Li JH, Riggan L, et al. The X-linked epigenetic regulator UTX controls NK cell-intrinsic sex differences. *Nat Immunol*. 2023;5(24):780–791. doi:10.1038/s41590-023-01463-8